IIETA International Information and Engineering Technology Association
Advancing the World of Information and Engineering

International Journal of Heat and Technology
Vol. 42, No. 6, December, 2024, pp. 1887-1900
Journal homepage: http://iieta.org/journals/ijht

Comparative Study of Hydration Kinetics in Binary and Ternary Cements Using the Avrami Model

Lila Kerrai[1], Samir Ladjali[2,3*], Samira Tebani[1]

[1] Laboratory of Reaction Engineering, Department of Chemical Engineering and Cryogenics, Faculty of Mechanical Engineering and Process Engineering, University of Sciences and Technology Hourai Boumedien (USTHB), El-Alia 16111, Algeria
[2] Process Engineering Department, Faculty of Science and Technology, Mustapha Stambouli University-Mascara, Mascara 29088, Algeria
[3] Laboratory of Materials Technology, Department of Chemical Engineering and Cryogenics, Faculty of Mechanical Engineering and Process Engineering, University of Sciences and Technology Houari Boumediene (USTHB), El-Alia 16111, Algeria

Corresponding Author Email: s.ladjali@univ-mascara.dz

https://doi.org/10.18280/ijht.420606

Received: 11 August 2024
Revised: 2 October 2024
Accepted: 10 October 2024
Available online: 31 December 2024

Keywords:
activation energy, degree of hydration, limestone, Portland cement, pozzolan

ABSTRACT

This study used a differential scanning calorimeter (DSC) in semi-adiabatic mode to investigate the hydration kinetics of binary and ternary cements, utilizing the Avrami-Kolmogorov model to determine key kinetic parameters. Two types of cement were developed: binary (made up of limestone and pozzolan) and ternary. To determine the most effective dosages, we compared the cements' physicochemical and mechanical properties to those of standard OPC cement (CEM I). The findings indicate that the presence of limestone in the cement has a negative effect on the residue on the sieve, thereby influencing the grinding process. After analyzing the three types of additives, we discovered that the optimal doses of limestone and pozzolan are 10%. The P10 mortar had the highest compressive strength (48.4MPa), followed by the L10 mortar (45.45MPa); the PL30 mortar had the lowest value of 40.7MPa, while the OPC cement reached 52.3MPa. DSC measurements of heat flow and hydration enthalpy show that the reference OPC cement has high values of Q_{max} (492.25 J/g) and ΔH (1513.6 J/g). The OPC cement has higher values of αmax (0.92) and Ea (45.818 kJ/g), followed by limestone and pozzolan cement. The lowest values are found in ternary cements. Thus, we determined that the optimal dosage for binary cement is 10% pozzolan and 10% limestone, and for ternary cement is 5% limestone and 25% pozzolan. The compressive strength, α_{max}, ΔH, Ea, and Q_{Max} were statistically analyzed using ANOVA. This analysis revealed that Q_{Max} and compressive strength have a significant impact on cement.

1. INTRODUCTION

Portland cement concrete is now the most widely used industrial material on the planet. Concrete's composition was generally limited to three components until the early 1930s: cement, water, and aggregates. To meet the diverse demands for concrete performance, various chemical and natural additions to modify specific properties were developed. Limestone, fly ash, pozzolan, and blast furnace slag are among the most commonly used additives [1, 2]. The advancement of scientific research in the field of cement has allowed us to discover new types of supplementary cementing materials, such as ternary cement, which is a cement that contains a mixture of two supplementary materials [3]. The addition of two types of additives to cement allows us to benefit from the properties of two additives at the same time, and the mortar produced by these two additives will be more durable and harder than cement with only one additive. Several studies have demonstrated that the incorporation of two admixtures in ternary cement can lead to the emergence of novel properties that were not observed in either of the individual admixtures [4, 5]. This finding can be explained by the fact that the admixtures can react with one another and produce new products that help to improve the performance of the cement. Other studies have shown that pozzolanic additions, such as natural pozzolan, play an important role when incorporated into OPC at a certain percentage [6], as they reduce permeability by modifying the pore structure, and the resulting concrete has significant resistance to reinforcement corrosion, acid attack, and sulfate attack. Hossain et al. [7] demonstrated that pozzolanic materials such as ground granulated blast furnace slag (GGBS), RHA, pulverized fuel ash (PFA), SF, FA, and POFA improve durability, reduce negative environmental effects, and lower the cost of concrete [8, 9]. According to Hale et al. [10], replacing cement with 25% slag and 15% FA improves the properties of both young and old concrete, including increased strength, decreased permeability, and decreased chloride penetration [11]. Several researchers [7] have also discovered a significant improvement in strength and porosity for ternary cement-mixed concretes [12]. Another observation has been made, according to which the inclusion of PFA and SF in concrete [13] as a partial replacement for cement reduces the concrete's chloride permeability. The hydration reaction is a series of extremely complex reactions that occur at the same time [14]. These reactions are caused by a significant release of heat via very exothermic and thermoactivated interactions between a powdery material composed of polyphase Portland cement grains and a liquid dispersion medium represented by the mixing water [15].

The dual actions of dissolution of the anhydrous cement phases and precipitation of the hydration products, with kinetics that vary over time, can be used to summarize the cement hydration process [12]. The mechanisms that determine reaction kinetics have been satisfactorily discovered thanks to microcalorimetry, but the mechanisms that determine them remain a source of contention. Exothermic heat is generated during cement hydration reactions, which raises the temperature of the concrete and speeds up the chemical hydration reactions. Concrete can crack if this heat is not controlled [15, 16]. The wall cools faster than the core in the cementitious matrix due to heat exchange with the external environment. These thermal gradients can cause concrete element cracking [17]. Hardened concrete's mechanical strength increases as the hydration process changes. Many factors will influence the dynamics of the hydration reactions, including the specific Blaine SSB surface area, particle size, chemical composition, water/cement ratio, mixing method, and the presence of added secondary elements (such as tuff, blast furnace slag, and pozzolan). If the contribution of these factors is not well controlled [18], the evolution of the kinetics may result in cementitious matrix degradation [19].

The cement hydration process is driven by very complex reactions in which several phases of clinker react at the same time. To better understand this phenomenon, many researchers have proposed mathematical functions for modeling the kinetics of cement hydration and its main phases. These models are distinguished by two key features: the conceptual model used to simulate the hydration process and the modeling scale used, which can be macroscopic or microscopic. In this case, the proposed laws are primarily empirical mathematical functions that accurately replicate the experimental curves. Reinhardt, for example, used heat release curves of hydration to model the evolution of hydration levels. Given this, our research has chosen to use the Avrami model, a macroscopic model that is especially well-suited for cement hydration reactions because it allows for a more general treatment of the reaction.

The Johnson-Mehl-Avrami-Kolmogorov equation, also known as the Avrami equation, was first empirically derived by Austin and Rickett to model ferrite decomposition [20, 21]. Subsequent derivations of this equation were used to simulate the rate of phase change in cast iron. Although this equation can also be considered a concentric growth model, we will treat it separately because it is commonly used in the cement industry. Indeed, it simulates the processes of nucleation and growth, in which small product nuclei form randomly in the pore space and build a complete skeleton at a constant rate across all available surfaces. This derivation assumes isotropic spherical growth of the nuclei and statistically explains the reduction in surface area caused by overlaps between neighboring nuclei.

We used two types of additives in this work, limestone and pozzolan, to make binary cement, and we mixed the two additives to make ternary cement. The effect of these additives on the physicochemical and mechanical properties, as well as the hydration mechanism of cement specimens prepared with these additives, was then studied. The substitution method was used to prepare the samples. Some of the clinker was replaced by pozzolan and limestone [21, 22] by varying the weight percentage of the additions. We conducted a quality control study in accordance with AFNOR standards, which included checking the mechanical performance of the mortar through compression, flexion, and water demand tests, as well as testing the residue on standard sieves to determine cement grindability [23]. To follow the kinetics of hydration, the heat of hydration was determined using semi-adiabatic calorimetry, and the Avrami model was used to determine the kinetic parameters, namely the degree of hydration, the rate constant, and the energy of activation.

2. MATERIALS AND METHODS

Clinker, limestone, pozzolana, and gypsum are sourced from the GICA group's Meftah cement plant in Algeria. After mixing the clinker, gypsum, and additive, we ground them in a ball mill to maintain a specific surface area (SSA) of 4000±50 cm^2/g per cement sample. Portland cement without additives, also known as OPC, is made up of 95% clinker and 5% gypsum. Pozzolan and limestone are additives that, at various mass percentages, replace a certain amount of clinker. Table 1 shows the masses of each constituent for one kilogram (1000 g) of each cement sample. The three pozzolan cement samples have different addition percentages of 10, 20 and 30% and are designated P10, P20 and P30, respectively. Three specimens of compound cement with limestone were prepared with different percentages of additions ranging from 10% to 30%, as indicated by the letters L10, L20, and L30.

Table 1. Mass % of additives in different cements

	OPC	**P10**	**P20**	**P30**	**PL10**	**PL20**	**PL30**	**L10**	**L20**	**L30**
%Clinker	95	84.904	74.808	64.712	60.112	59.95	59.8	85	74.920	65.051
%Pouzolan	-	10	20	30	10	20	30	-	-	-
%Limstone	-	-	-	-	25	15	5	10	20	30
%Gypsum	5	5.096	5.192	5.280	4.888	5.050	5.200	5	5.071	4.949
Mass(g)	**OPC**	**P10**	**P20**	**P30**	**PL10**	**PL20**	**PL30**	**L10**	**L20**	**L30**
Clinker	950	849.04	748.08	647.12	601.12	599.5	598.	850	749.20	650.51
Pozzolan	-	100	200	300	100	200	300	-	-	-
Limestone	-	-	-	-	250	150	50	100	200	300
Gypsum	50	50.96	51.92	52.80	48.88	50.50	52.0	50	50.71	49.49
SSB (cm^2/g)	3985	3979	4015	3957	4023	3981	4014	3990	3994	3990

Table 2. Composition oxides (in mass %) of clinker, limestone, pozzolan and gypsum

%	Clinker	Pouzolan	Limestone	Gypsum
SiO_2	22.33	1.83	45.64	8.08
Al_2O_3	5.19	0.84	18.54	2.50
Fe_2O_3	3.25	0.00	12.72	1.12
CaO	65.49	51.23	9.27	27.01
MgO	0.97	0.19	4.21	4.70
SO_3	0.31	0.39	0.01	31.56
K_2O	0.64	0.09	1.94	0.37
Na_2O	0.25	0.00	3.64	0.00
$(CaO)_{free}$	1.11	-	-	-
Fire loss	0.19	41.63	3.29	22.86

Table 3. Composition oxides (in mass %) of cements

%	OPC	P10	P20	P30	PL10	PL20	PL30	L10	L20	L30
SiO_2	21.20	22.75	25.38	27.47	18.41	22.71	27.21	19.28	17.03	14.66
Al_2O_3	5.01	6.07	7.41	8.37	5.15	6.70	8.45	4.34	3.95	3.53
Fe_2O_3	3.46	4.11	4.95	5.73	2.10	4.49	5.56	2.93	2.69	2.41
CaO	64.89	57.67	53.29	47.26	55.16	50.31	47.69	63.82	64.06	64.53
MgO	1.22	1.43	1.76	2.03	1.25	1.57	2.05	1.00	0.93	0.84
SO_3	1.81	1.81	1.81	1.81	1.81	1.81	1.81	1.61	1.74	1.77
K_2O	0.70	0.85	0.97	1.03	0.67	0.83	1.10	0.61	0.56	0.54
Na_2O	0.07	0.26	0.28	0.36	0.15	0.22	0.66	0.11	0.09	0.06
$(CaO)_{free}$	1.37	1.24	1.18	0.65	0.68	0.75	0.82	0.56	0.95	0.82
Fire loss	1.34	1.96	2.17	2.31	11.65	8.08	4.43	6.085	9.8	14.07

Table 4. Mineralogical composition of clinker

Mineralogical Phase	C_3S	C_2S	C_3A	C_4AF
Mass fraction	57.39	21.05	8.25	9.89

Table 1 also shows three samples of ternary cement with a 35% addition of a mixture of pozzolan and limestone labeled PL10, PL20, and PL30. The X-ray Fluorescence device (XRF) was used to determine the chemical composition of clinker, cement, gypsum, and oxides. The equipment used is the Cubix XRF Panalytical (Tables 2 and 3). The Bogue formula was used to determine the mineralogical composition of the clinker illustrated in Table 4.

The SSB was measured using a Blaine-meter of type TONI PERM, and the residues on the sieve were measured using a standard sieve of 45 and 90 µm and a HOSOKAWA ALPINE apparatus. Standardized mechanical (ensile and compressive strengths) tests were performed on a TONI PRAX press at 2, 7, and 28 days to track the evolution of performance. Each specimen provides one flexural and two compressive results, with the compressive strength calculated as the average of two measurements. The test examines the tensile and compressive strengths of standard mortar, with the only variable being the nature of the hydraulic binder, allowing the mortar's strength to be related to that of the cement.

The compressive and flexural strengths were measured using mechanically compacted prismatic specimens measuring 4 cm×4 cm and 16 cm in length, following the NA 234 standard. After 24 hours of storage under plastic film, the samples were demolded and placed in water in the laboratory. Calorimetry measures heat release as a function of time or temperature, depending on the mode (semi-adiabatic or isothermal) and various factors such as particle size, chemical composition, E/C ratio, and sample temperature. The semi-adiabatic calorimeter used in this study enables precise measurement of heat release during cement sample hydration under controlled conditions. This device maintains partial thermal insulation, reducing heat exchange with the environment while measuring temperature and heat variations caused by chemical reactions. The collected data enables the analysis of heat peaks, which are critical for understanding the cement's hydration mechanisms and performance. The calorimeter, which is controlled by a computer, records the sample's behavior, with peaks on the thermograms indicating thermal effects; a higher peak intensity indicates more heat release. The differential scanning calorimeter (DSC) detects the difference in enthalpy between a sample and a reference as a function of temperature, with the DSC signal representing the enthalpy derivative over time. The laboratory has a Perkin Elmer Pyris 6 DSC cell that operates from 123 to 998K with a 0.1K accuracy. The cell is linked to a PC for automatic data collection and is constantly purged with dry nitrogen to avoid any interaction with the furnace atmosphere. **Sample Preparation (**see Figure 1**)**: Step 1 involves weighing 1 g of cement and measuring a corresponding amount of water with a micropipette. After manually mixing the two for one minute to form a paste (step 2), we pour a portion of the paste into an aluminum pellet (step 3), making sure it does not exceed 10 mg (step 4). We analyzed the samples at heating (step 5) rates ranging from 1 to 10°C/min, with the optimal rate being 10°C/min, revealing a clear peak between 80 and 150°C for all samples (see Figure 2). This heating rate allows for 30 minutes of hydration to investigate how the dormant period affects hydration kinetics, while sample warming results in a short setting time. A semi-adiabatic calorimeter is used to measure the heat of hydration under semi-adiabatic conditions, with a heating rate of 10°C/min between 20°C and 250°C. The study aims to analyze how temperature affects hydration kinetics, including Q_{max}, αmax, enthalpy variation, and activation energy. Integrating the heat flux over time yields heat release curves.

$$Q(t) = \int_0^t \frac{dQ}{dt} dt \tag{1}$$

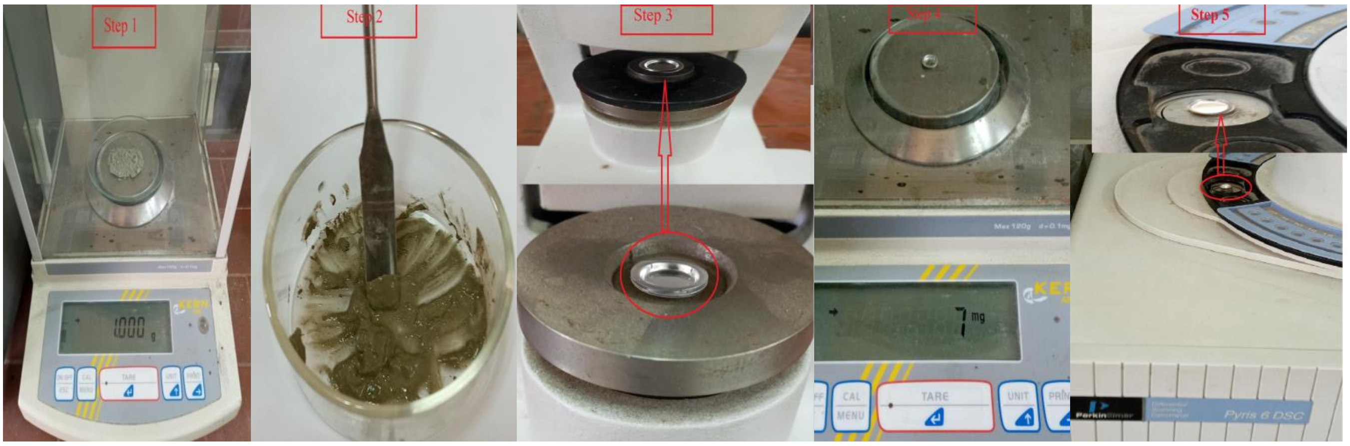

Figure 1. Sample preparation of cement paste

Figure 2. Photograph of the DSC measurement device: 1: Nitrogen gas bottle; 2: Perkin Elmer DSC; 3: Microcomputer with Pyris 6 software)

Eq. (2) was used to calculate the degree of hydration:

$$\alpha_{(t)} = \frac{Q_t}{Q_\alpha} \tag{2}$$

The velocity constants K were calculated using the Avrami-Kolmogorov [24, 25] Eq. (3):

$$\begin{gathered} -ln(1-\alpha) = kt^n \\ \ln(-(\ln(1-\alpha) = lnk + nln(t) \end{gathered} \tag{3}$$

Eq. (4) was used to calculate the apparent activation energy [26]:

$$\ln k = a - \frac{E_a}{RT} \tag{4}$$

3. RESULTS AND DISCUSSION

3.1 Residue on standard sieves

Figures 3 and 4 depict the evolution of residue on 45 and 90 µm sieves as a function of pozzolan and limestone addition percentages. This figure shows that even when the percentage of pozzolan addition is changed, the residue on the sieves remains nearly constant, indicating that the pozzolan has no effect on the residue on sieves, which can be explained by the fact that the pozzolan prevents clinker agglomeration during grinding [24]. However, as the percentage of limestone increases, so does the residue [22], implying that grinding the clinker with limestone adds coarser particles, which increases the residue on the sieve [27]. Limestone has a negative effect because it causes the clinker to agglomerate [28]. Similar results were obtained by Gupta et al. [29]. However, Turanli's work [30] confirms that, in terms of particle size distribution, blended cements containing large quantities of pozzolan and produced using a laboratory-type mill have a coarser texture than reference Portland cement.

3.2 Compressive strengths and flexural strengths

Figure 5 depicts the effect of pozzolan and limestone substitution rates on the compressive strength of mortars of various ages. Figure 5 shows that regardless of the type of addition or the rate of substitution, all of the mortars in the cement developed compressive strengths lower than the reference mortar at all ages [31]. As can be seen, the decrease in strength is proportional to the increase in addition [32]. It can also be noted that the limestone combination has a significant effect on the compressive strength of L10, L20, and L30 mortars at various ages. In fact, the drop in strength compared to the reference is significant at 2 and 7 days and is estimated at 2 days to be 21.96%, 39.607%, and 44.313 for

10%, 20%, and 30% substitution, respectively (Table 5). Boubekeur et al. [33] discovered that increasing the percentage of limestone from 10% to 20% reduced compressive strength by 11% and 20%, respectively, when compared to the reference mortar. S. Mansour demonstrated in his study that the substitution of 10% limestone reduced the strength of mortars by 5% after 2 days when compared to the control mortar. At 2 days, the difference in strength drop is negligible compared to the 50% drop for a 20% limestone substitution, making it comparable to that of the reference mortar, as observed by Elkhadiri and Puertas [34]. Diab et al. [35], on the other hand, it was confirmed that using up to 10% limestone does not significantly reduce the properties of the concrete.

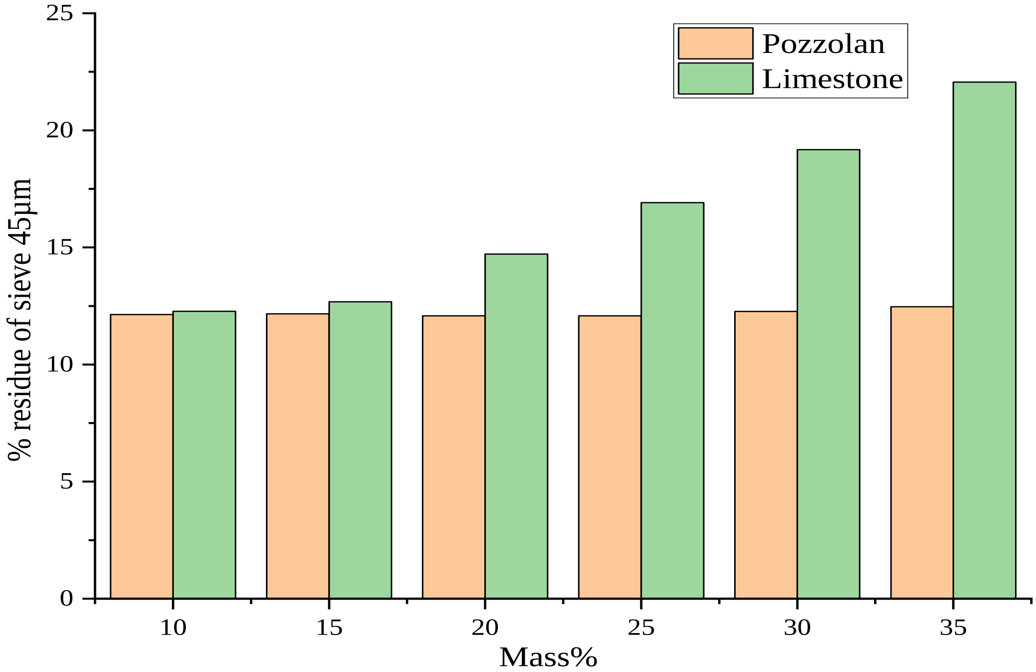

Figure 3. Evolution of residue on 45 µm standardized sieve to the percentage of additions

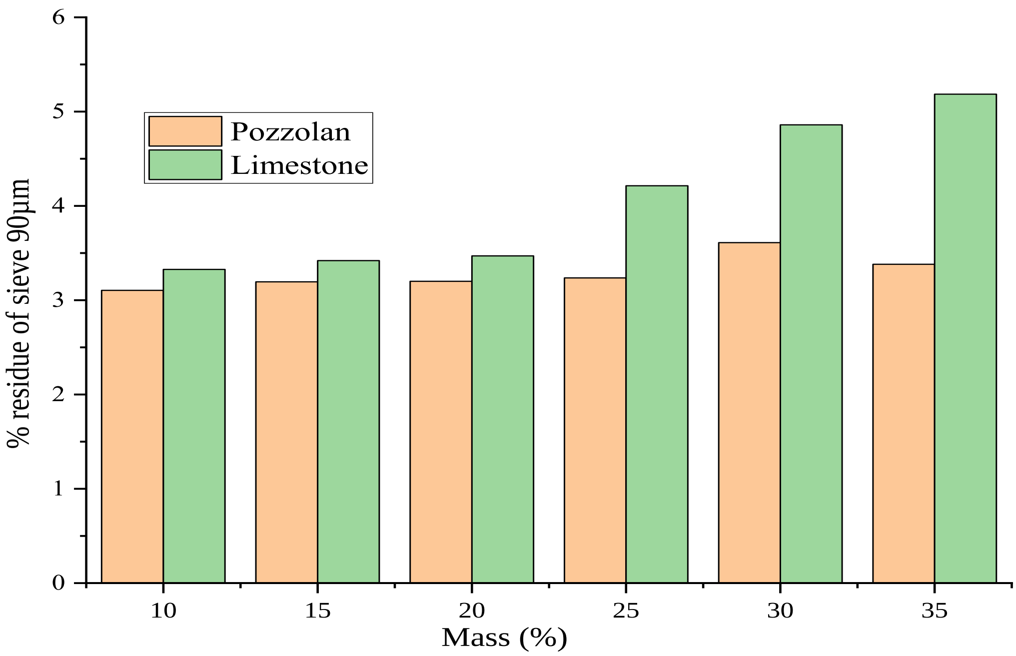

Figure 4. Evolution of residue on 90 µm standardized sieve to the percentage of additions

Table 5. Average deviations between compressive strengths of the cements and compressive strength of OPC

%	P10	P20	P30	PL10	PL20	PL30	L10	L20	L30
2 days	12.470	39.607	27.764	34.313	36.274	46.941	21.960	39.607	44.313
7 days	11.266	23.517	28.326	10.693	28.669	39.088	10.006	26.837	34.623
28 days	7.456	14.531	19.120	22.179	25.430	35.946	13.097	25.430	31.548

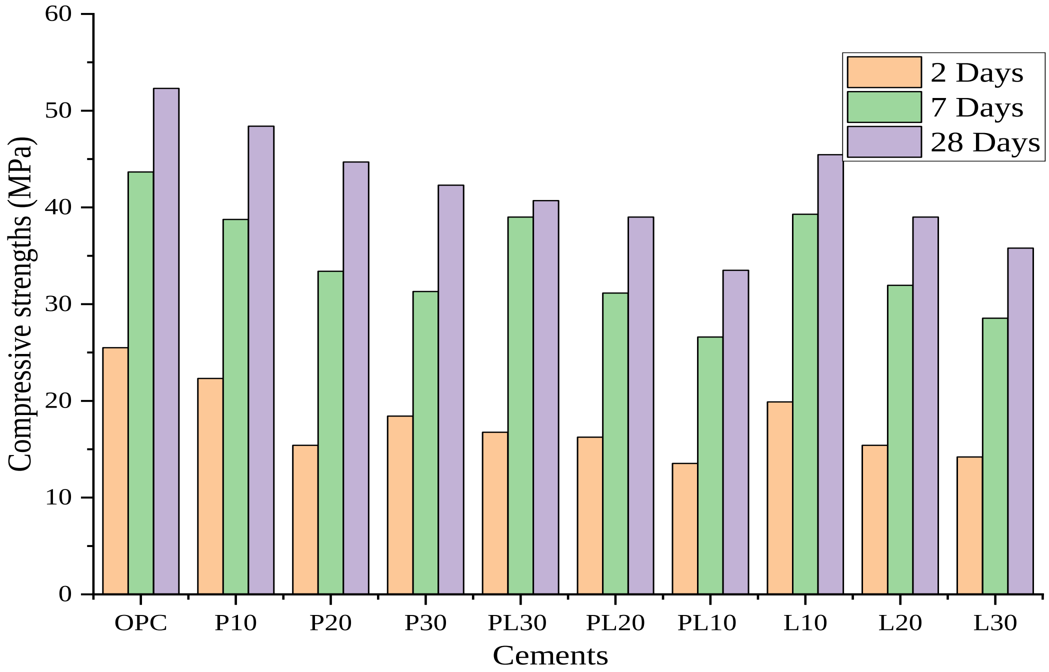

Figure 5. Evolution of the compressive strengths according to the age of the mortars

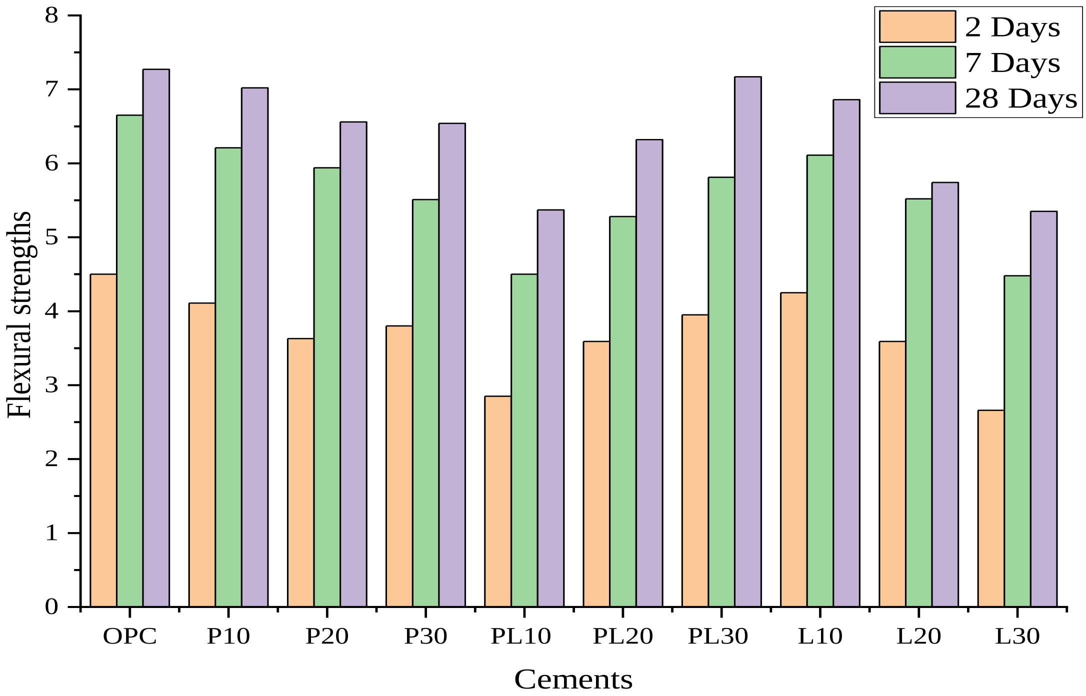

Figure 6. Evolution of the flexural strengths according to the age of the mortars

Table 6. Average deviations between compressive strengths of the cements and flexural strength of OPC

%	P10	P20	P30	PL10	PL20	PL30	L10	L20	L30
2 days	8.667	19.333	15.556	36.667	20.222	12.222	5.556	20.222	40.889
7 days	6.617	10.677	17.143	32.331	20.602	12.632	8.120	16.992	32.632
28 days	3.439	9.766	10.041	26.135	13.067	1.376	5.640	21.045	26.410

In general, concretes based on Portland limestone cement (PLC) with up to 10% limestone exhibit competitive properties when compared to Portland cement concretes. In contrast, adding a higher percentage of limestone to the cement reduces the performance of the concrete. According to several researchers, this approach of resistance at a young age for the reference mortar and the one containing 10% limestone can be attributed to the reaction that occurs between limestone and C_3A of the OPC cement to form a hydrated calcium carboaluminate that precipitates in the pores, as well as the acceleration of C_3S hydration due to the presence of limestone particles. However, some researchers have developed alternative addition rates. For example, Turanli et al. [30] discovered that a mortar containing 20% limestone was the most effective. This contradicts Turanli's [30] findings, which showed that increasing the pozzolan content to 35%, 45%, and 55% improves cement performance, particularly compressive and flexural strength. According to his findings, adding pozzolan at these concentrations improves the cement's structure, resulting in greater mechanical resistance.

This difference could be explained by a variety of factors, including the quality of the pozzolan used, the mixing and curing conditions, or the specific proportions of other components in cement formulations. It is critical to note that the performance of different cements can vary depending on the nature of the materials and production techniques, emphasizing the importance of conducting additional research to establish clear recommendations for the use of pozzolan in cements.

For all ages, the compressive strengths of mortars made with various pozzolan substitution rates are always lower than those of the reference mortar. Increased pozzolan dosage has a negative effect on compressive strength at an early age: it goes from a difference of 12.47% to 27.724% at the age of 2 days compared to the reference for pozzolan dosages ranging from 10 to 30%. This difference tended to decrease over time, rising from 7.456% to 14.531% at 28 days of age for the same substitution rates (10-30%), indicating that the pozzolan rate has a long-term positive effect (see Table 5). The pozzolanic activity of the natural pozzolan addition, which consists of fixing the portlandite Ca $(OH)_2$, released by the hydration of the OPC, gives rise to additional, second-generation hydrated calcium silicates CSH, occupying a large space in the cementitious matrix and thus contributing to the development of strength, is the most effective for long-term mortar strength (28 days). This increase in compressive strength is consistent with NA 234, which defines pozzolans as siliceous or silico-aluminous materials with an inherent pozzolanic activity that increases with age and is only effective after 28 days [36].

Furthermore, this discovery demonstrates that the activity of natural pozzolans is extremely slow. This effect is due to the fact that the pozzolanic reaction continues its effect in the long term by forming a second additional CSH, which increases with the dosage of pozzolanic addition. Figure 3 depicts the effect of the combination (pozzolan+limestone) on the compressive strength of mortars at various ages. At all ages, the strength of mortars tends to decrease as the percentage of pozzolan decreases and the percentage of limestone increases, resulting in the non-beneficial effect of incorporating the latter. The decrease in compressive strength of mortars containing both pozzolan and limestone can be attributed, on the one hand, to the limestone's contribution to accelerating cement hydration and, on the other, to the pozzolanic reaction of the pozzolan [37, 38]. Grace's research demonstrated that a low level of pozzolan replacement in a ternary mortar containing both limestone and pozzolan can result in maximum strength.

In contrast, this study found that a high pozzolan content improves the performance of the cement. The specific interactions of the components in the studied formulations could explain this difference. In the case of Ghrici et al. [39], the synergistic effect at low pozzolan content appears to optimize the mortar's structure, whereas the current study shows that higher pozzolan proportions increase the mechanical strength of the cement by promoting more advantageous chemical reactions. It would be interesting to investigate the underlying mechanisms behind these observations further, particularly in terms of particle size distribution and material reactivity. This could provide valuable information about how different material combinations affect the final properties of cement and concrete.

Figure 6 depicts the effect of pozzolan, limestone, and a limestone-pozzolan mixture on the flexural strength of mortars at different ages: 2, 7, and 28 days. At ages 2 and 7 days, there is a systematic decrease in mortar strength. This strength tends to improve in the long term at 28 days as the percentage of pozzolan increases. Figure 6 shows that mortar containing 10% limestone and 10% pozzolan appears to perform best in terms of compressive strength. However, the combination of 5% pozzolan + 30% limestone produces results similar to those of the best-performing ternary mortar discovered by Lollini et al. [40]. The incorporation of limestone at a rate of 5 to 30% reduces the flexural strength of mortars containing natural pozzolan at an early age (2 and 7 days). This resistance improves after 28 days with the pozzolan combination [41] (30% pozzolan and 5% limestone), which appears to perform best, reaching 98% of the reference mortar see Table 6.

3.3 Heat flow

The evolution of heat flow induced by hydrated limestone-based cement is depicted in Figure 7. The heat flow released by the L10 limestone cement is greater than that of the reference cement. Because the L20 cement has a heat flow that is close to the reference, increasing the limestone content reduces the heat released during the hydration reaction. The limestone cement reaches the peak before the reference cement; the L10 and L20 cement reach the peak after 9 minutes, while the L30 cement reaches the peak after 7 minutes. This is due to the presence of limestone in the cement, which accelerates the hydration reaction. Aqel et al. [17, 42] reported the same results.

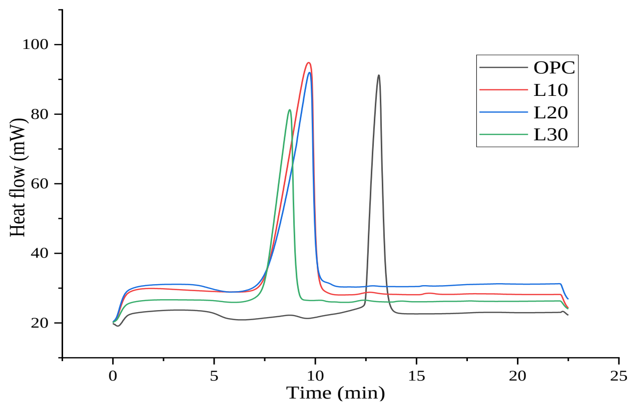

Figure 7. Evolution of heat flow as a function of time of cement with limestone

The evolution of the heat flow induced by pozzolan-based hydrated cement is shown in Figure 8. The heat flow released by the P10 pozzolan cement exceeds that of the reference cement P20, giving a heat flow close to the reference, the same behavior as adding limestone, so increasing the pozzolan content in the cement decreases the heat flow. Because the presence of pozzolan accelerates the hydration reaction, the P10, P20, and P30 cements reach the peak after 11, 9, and 8 minutes of repetition, respectively, compared to 13 minutes for the cement OPC. Wang et al. [43] observed an acceleration in the hydration reaction of pozzolan-containing cement. Celik et al. [44] demonstrated that replacing 30% and 50% pozzolan increases setting time, whereas replacing 15% pozzolan has no effect on setting time. Figure 9 depicts the evolution of the heat flux induced by the ternary cement composed of pozzolan and limestone. The heat flux emitted by the PL10 and PL20 cement exceeds that of the reference cement, exhibiting the same behavior as the addition of limestone and pozzolan, the pozzolan and limestone mixture, and the hydration reaction as the PL10, PL20, and PL30 cement [41].

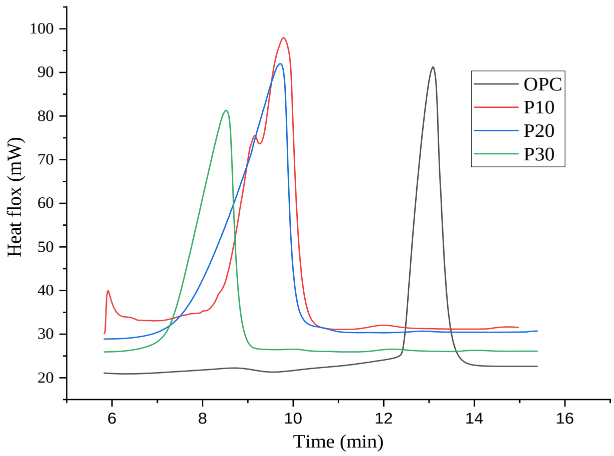

Figure 8. Evolution of heat flow as a function of time of cement with pozzolan

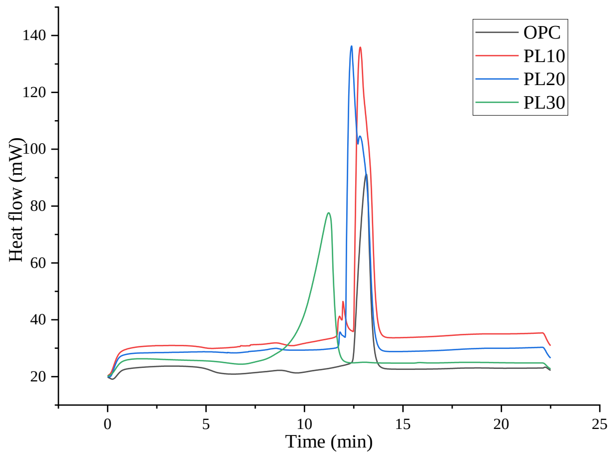

Figure 9. Evolution of heat flow as a function of time of cement with pozzolan and limestone

3.4 Degree of hydration

Figures 10, 11, and 12 show a detailed progression of the degree of hydration of different cements over time. These illustrations clearly demonstrate that, regardless of the type of cement used, all go through three phases of hydration: dormancy, acceleration, and hardening and curing [45]. The dormant period, characterized by low chemical activity, is critical for the development of the cement's mechanical properties. It is worth noting that the reference cement has the highest degree of hydration, indicating a faster chemical reactivity than the other tested cements. In contrast, the presence of limestone and pozzolan in the mixtures tends to extend this dormant period, resulting in a longer setting time for the formulations L10, L20, P10, P20, and P30. This can be attributed to the dilution effect and the alteration of the interactions between cement particles and additives.

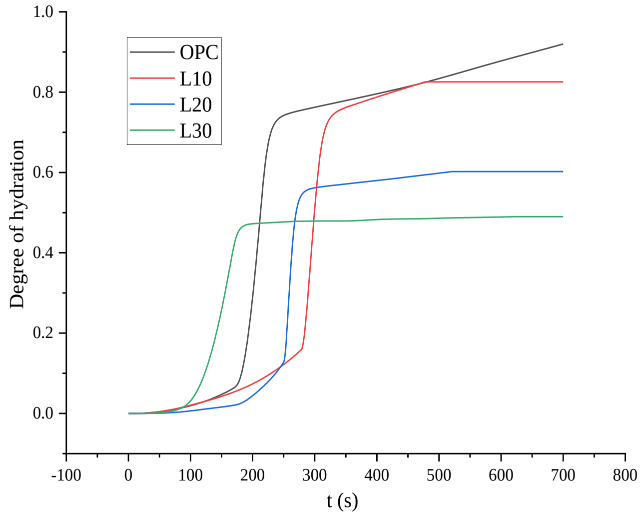

Figure 10. Evolution of degree of hydration as a function of time of cement with limestone

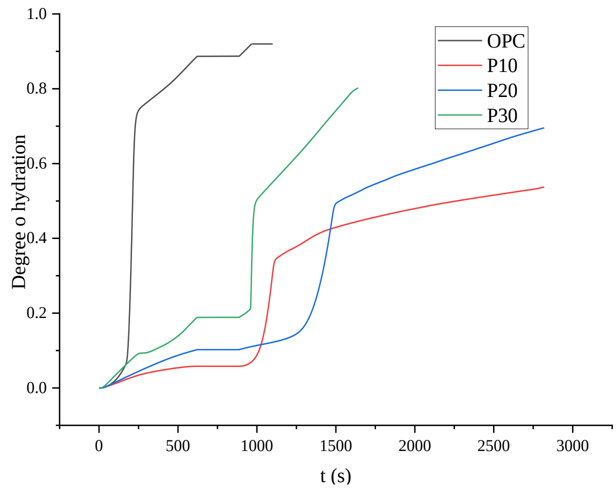

Figure 11. Evolution of degree of hydration as a function of time of cement with pozzolan

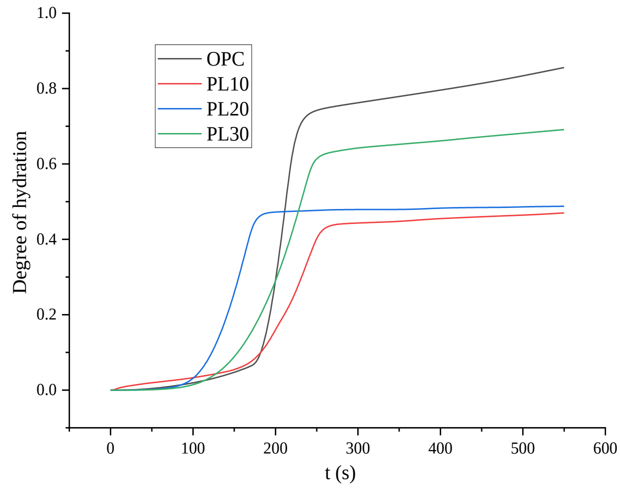

Figure 12. Evolution of degree of hydration as a function of time of cement with limestone and pozzolan

However, the ternary cement, which combines pozzolan and limestone, has a shorter setting time than the PL10 cement. This suggests that the combination of the two materials can result in a synergy that promotes faster hydration, most likely due to the heterogeneous nucleation effect. According to de Siqueira and Cordeiro [46], this effect helps to accelerate hydration during the first few days, allowing for better integration of the elements into the cement matrix. Despite the initial acceleration, compressive strength decreases on days 7, 28, and 90. This decline may be due to the dilution effect, in which the addition of inert materials such as limestone and pozzolan reduces the concentration of reactive phases, lowering the final strength of the concrete.

3.5 Parameters

DSC was used to determine enthalpy, which is shown in Table 7. Heat flux integration Eq. (1) determines the hydration heat, as shown in Table 7. Eq. (2) determines the degree of hydration, which is shown in Table 7. Eq. (3) determines the Avrami equation and rate constant, which are shown in Table 7. Eq. (4) calculates the activation energy, which is shown in Table 7. The values in Table 7 show that all of the correlation coefficients are in the order of 0.99, which explains the validity of the Avrami model for determining the kinetic parameters. Table 7 shows that the maximum heat Q_{max}=492.5 J/g, the degree of hydration α_{max}=0.92, the enthalpy ΔH=-1513.6 J/g, the average rate constant K_{moy}=6.67×10^3. These findings emphasize the significance of cement composition and interactions between different materials in the development of mechanical properties in hydrated cements. A better understanding of these dynamics may lead to the optimization of cement formulations, promoting improved performance in practical applications [47, 48]. The activation energy Ea of Portland OPC cement without additives, measured at 45.818 J/g, is significantly higher than that of cement containing additives. This observation emphasizes the need for additional components in the hydration process. The values obtained for pozzolan cement are comparable to those of the reference cement, which supports Kerrai et al.'s conclusions.

According to Lila et al. [27] and Wang [49], cements without additions produce the highest levels of released heat (Qmax) and activation energy (Ea). Furthermore, increasing the limestone content in ternary cement has a direct impact on thermal properties. This increase decreases Qmax, αmax, enthalpy ΔH, and the mean velocity constant Kmoy. This suggests that the amount of added limestone has an inverse relationship with heat generation and hydration. The clinker's mineralogical composition may influence the hydration reaction [50, 51]. When these phases in the composite cement are reduced, heat is released less efficiently. This dynamic emphasizes the importance of mineral composition in developing the thermal and hydration properties of different cements, highlighting the critical role of materials in optimizing their performance.

Table 7 shows that the activation energy values for cement with limestone are higher than those for ternary cement (limestone+pozzolan). It has been demonstrated that the activation energy released by cement based on a mixture of limestone and pozzolan decreases as the percentage of these additions in cement increases and that 10% substitution is the most effective for all cement, with similar results found for the compressive and flexural strength of cement [52]. The calculated apparent activation energies for alite of 32-34 kJ/mol agree with previous studies that reported values ranging from 26 to 42 kJ/mol [53]. Research has shown that as the proportion of limestone and pozzolan additions increases in the cement mix, the activation energy released decreases. This trend indicates that the interactions between these materials during the hydration process become more efficient, leading to a more favorable reaction environment.

Notably, a substitution level of 10% has been identified as the most effective across all cement types studied. This optimal percentage appears to enhance the mechanical properties of the cement, as similar improvements have been reported in both compressive and flexural strength. The calculated apparent activation energies for alite, ranging from 32 to 34 kJ/mol, align well with previous studies that reported values between 26 and 42 kJ/mol., This consistency across different research efforts strengthens the validity of the findings and emphasizes the relevance of alite's role in cement hydration. Alite, being a major component of Portland cement, significantly affects the kinetics of hydration and the development of strength in the cement matrix. Overall, these insights underscore the importance of carefully selecting and optimizing the mineral components in cement formulations to achieve desired performance characteristics. The relationships between activation energy, the composition of the cement, and the resultant mechanical properties are crucial for advancing the understanding and application of modern cement technology.

3.6 Statistical analysis of results

We used Minitab to perform a statistical analysis, including an ANOVA test with Tukey's test on compressive strength, to investigate the kinetic evolution of hydration advancement degrees, as well as enthalpy and activation energy. The purpose of this study is to assess the impact of each parameter on the behavior of the cement.

Table 7. Q_{max}, ΔH, α_{max}, k_{moy}, E_a, R^2 and Avrami adjustment equation for various cements

Cement	Q_{Max} (J/g)	ΔH_R (J/g)	α_{max}	$k_{moy} \times 10^3$	E_a (kJ/g)	Avrami Adjustment Equation	R^2
OPC	492.5	-1513.6	0.92	6.67	45.818	y=2.2294x-14.196	0.990
P10	460.9	-1437.1	0.53	3,62	36.077	y=2.1189x-5.1982	0.997
P20	450.8	-1359.2	0.72	3,32	35.326	y=0.9105x-8.0914	0.990
P30	440.7	-1279.3	0.8	3,12	30.042	y=2.3317x-14.772	0.994
PL10	437.3	-1051.6	0.47	3.12	29.973	y=2.469x-17.078	0.997
PL20	445.7	-1136.0	0.49	3.32	27.673	y=1.0974x-8.448	0.998
PL30	459.1	-1183.2	0.69	2.88	21.201	y=2.4902x-16.674	0.993
L10	460.57	-1470.9	0.83	2.7	43.62	y=2.3317x-14.772	0.994
L20	420.11	-1411	0.60	2.53	37.18	y=2.489x-17.119	0.997
L30	300.14	-1248.2	0.49	1.88	26.85	y=1.0974x-8.448	0.998

Table 8. Tukey simultaneous tests for differences of means (compressive strength)

Level Difference	Mean Difference	SE Difference	95% CI	T-Value	Adjusted P-Value
Days 7-Days 2	16.60	2.28	(10.95, 22.25)	7.29	0.000
Days 28-Days 2	24.35	2.28	(18.70, 30.00)	10.70	0.000
Days 28-Days 7	7.75	2.28	(2.10, 13.40)	3.40	0.006

Individual confidence level=98.04%

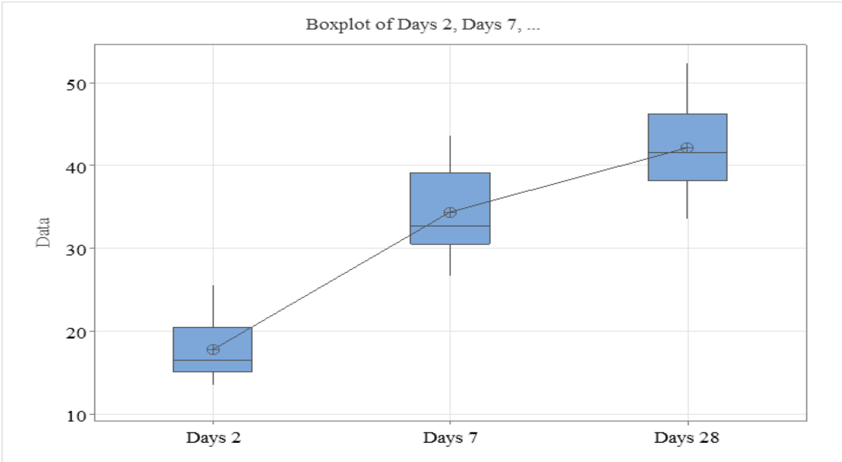

Figure 13. Boxplot of compressive strength at 2 days, 7 days and 28 days

Table 9. Tukey simultaneous tests for differences of means (ΔH, Q_{Max}, α_{max}, Ea and Days 28)

Difference of Levels	Difference of Means	SE of Difference	95% CI	T-Value	Adjusted P-Value
ΔH-Q_{Max}	-1745.8	32.6	(-1838.4, -1653.2)	-53.59	0.000
α_{max}-Q_{Max}	-436.1	32.6	(-528.7, -343.5)	-13.39	0.000
Ea-QMax	-403.4	32.6	(-496.0, -310.8)	-12.38	0.000
Days 28-Q_{Max}	-394.7	32.6	(-487.3, -302.1)	-12.11	0.000
α_{max}-ΔH	1309.7	32.6	(1217.1, 1402.3)	40.20	0.000
Ea-ΔH	1342.4	32.6	(1249.8, 1435.0)	41.20	0.000
Days 28-ΔH	1351.1	32.6	(1258.5, 1443.7)	41.47	0.000
Ea-α_{max}	32.7	32.6	(-59.9, 125.3)	1.00	0.852
Days 28-Alpha	41.5	32.6	(-51.1, 134.1)	1.27	0.709
Days 28-Ea	8.7	32.6	(-83.9, 101.3)	0.27	0.999

3.6.1 Compressive strength

Table 8 shows the results of the ANOVA test on the compressive strength of all cements at various ages. Significant differences are observed between days 2 and 7, as well as between Value 1 and Value 3, with adjusted p-values of 0.000. This provides strong evidence that the means of these groups differ. The difference between days 7 and 28 is also significant (p=0.006), albeit less pronounced than the previous two comparisons.

Day 28 has the highest mean compared to days 2 and 7, with a 24.35 difference from day 2. This suggests that Value 3 has a stronger positive effect on the measured variable. The 95% confidence intervals for all comparisons do not include zero, indicating that the observed differences are statistically significant and not due to chance. These findings indicate that the values of the compared groups have significant and varying effects on the measured variable. The greatest impact seems to be on day 28, while the lowest value is on day 2. This may have significant implications for your research or application.

Figure 13 of the boxplot shows significant differences between the three periods, with medians trending upward from Days 2 to 28. The data's variability appears to be increasing, which could indicate a greater dispersion of measured values in later periods. This indicates an upward trend and implies that the measured values will increase over time.

3.6.2 Kinetic parameter

Based on previous findings, it is clear that 28-day strength is the most important parameter. We will compare this strength to other parameters, including ΔH, Q Max, αmax, Ea, and Days 28. This analysis will allow us to determine the impact of each of these variables on the cement's performance.

Table 9 reveals significant differences between Q Max and other parameters, including ΔH, Alpha, Ea, and Days 28. There is no significant difference between the comparisons "Ea - Alpha" (P=0.852), "Days 28-Alpha" (P=0.709), and "Days 28-Ea" (P=0.999). This suggests that the means of these groups are comparable. Results indicate that Q_{Max} is significantly higher than ΔH, Alpha, Ea, and Days 28. However, there is no significant difference between Ea, Alpha, and Days 28.

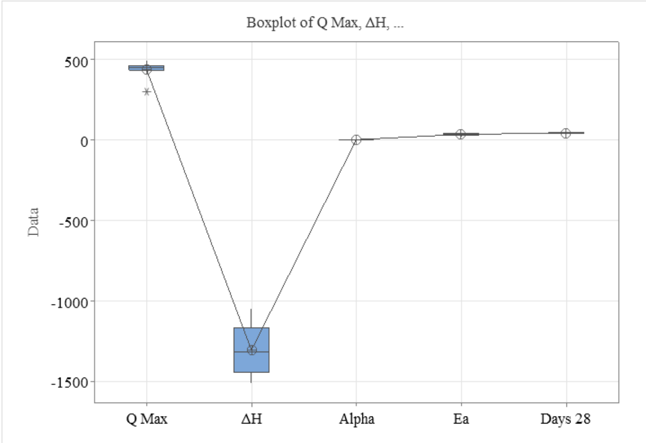

Figure 14. Boxplot of compressive strength: Q Max, ΔH, Alpha, Ea, and Days 28

These findings indicate that Q Max has a significant impact when compared to the other studied parameters. Figure 14 displays an interval plot with 95% confidence intervals for the means of the variables (Q Max, ΔH, Alpha, Ea, and Days 28). The graph clearly shows that Q Max is the most performant parameter, and ΔH is the least performant. The results also show that Q Max has a significant influence when compared to the other parameters, which perform similarly. As for Ea, the mean for Days 28 is also close to zero, implying that its performance is comparable to that of Ea.

4. CONCLUSION

The 45 and 90 µm sieves show that pozzolan prevents clinker agglomeration during grinding, whereas limestone causes it by producing coarser particles and increasing residue. The study of the effect of additives on compressive and flexural strengths reveals a systematic decrease in mortar strengths at early ages (2 and 7 days) as the percentages of pozzolan, limestone, and the limestone-pozzolan combination increase. The decrease in strength compared to the reference mortar (OPC) is observed to diminish over time, indicating that mechanical properties improve gradually as the mortar ages. The decrease in mortar strength tends to subside after 28 days, indicating that pozzolan has a long-term beneficial effect over other components, particularly limestone and the limestone-pozzolan combination. This observation emphasizes the importance of pozzolan in cement formulation, as it promotes long-term durability and strength. For long-term mortar strengths (28 days), the substitution of 10% pozzolan is especially effective. This optimal rate provides superior mechanical performance, even when compared to formulations containing only limestone. This suggests that pozzolan not only improves the mortar's initial strength but also its long-term behavior, which is critical for use in demanding environments.

In contrast, an examination of ternary cements, which contain both limestone and pozzolan, reveals a concerning trend. The mortars' strength decreases as the percentage of pozzolan decreases and that of limestone increases. This results in a non-beneficial effect from the incorporation of limestone, implying that increasing its proportion in the formulation may compromise the mortar's mechanical properties.

The experiments carried out under semi-adiabatic conditions, with a temperature range of 20 to 250°C and a heating rate of 10°C/min, revealed that, regardless of the type of cement, the evolution of the degree of hydration over time follows similar patterns. The hydration mechanism of Portland cement is divided into three essential phases: the dormant period, the acceleration period, and the slowdown and hardening period. It is worth noting that when the substitution rate of additives in cement is high, the degrees of hydration, rate constants, and activation energies are generally lower, which is consistent across all cements studied. Portland pozzolan cement, in particular, stands out for having higher hydration levels, rate constants, and activation energies than limestone cement or ternary cement blocks. This finding emphasizes the effectiveness of pozzolan as an additive, which contributes to improved long-term mechanical performance.

In light of the findings, it is critical to conduct regular studies and tests under semi-adiabatic conditions in the cement industry. This will provide a better understanding of the hydration behavior of various cement formulations. Indeed, continuous evaluation will help to optimize formulations and improve the ability to predict performance under a variety of environmental conditions. This approach will help to improve the durability and efficiency of cement products. The statistical results from the ANOVA test with Minitab show significant differences between the periods, with medians trending upward and data variability increasing over time. This implies that the measured values become higher and more dispersed as the days pass. The results also show that Q Max has a significant influence when compared to the other parameters, which perform fairly similarly.

ACKNOWLEDGEMENTS

The authors would like to acknowledge the laboratory Reactions and Process Engineering and the Department of Chemical Engineering and Cryogenics for financial support. The authors would like to acknowledge the Algeria cement plant of Meftah for the raw materials and analysis of XRF, water demand for normal consistency, setting time and mechanical test.

REFERENCES

[1] Ardoğa, M.K., Erdoğan, S.T., Tokyay, M. (2019). Effect of particle size on early heat evolution of interground natural pozzolan blended cements. Construction and Building Materials, 206: 210-218. https://doi.org/10.1016/j.conbuildmat.2019.02.055

[2] Vassilev, S.V., Baxter, D., Andersen, L.K., Vassileva, C.G. (2010). An overview of the chemical composition of biomass. Fuel, 89(5): 913-933. https://doi.org/10.1016/j.fuel.2009.10.022

[3] Marrok, S., Belachia, M., Kherraf, L., Salhi, M., Khaldi, N. (2024). Investigating the impact of stainless steel shavings fibers 316L on enhancing the properties of high-flow sand concrete in the long-term. Annales de Chimie Science des Matériaux, 48(4): 529-537. https://doi.org/10.18280/acsm.480410

[4] Tchamdjou, W.H.J., Cherradi, T., Abidi, M.L., de Oliveira, L.P. (2017). Influence of different amounts of natural pozzolan from volcanic scoria on the rheological

properties of Portland cement pastes. Energy Procedia, 139: 696-702. https://doi.org/10.1016/j.egypro.2017.11.274
[5] Ahmad, S., Lawan, A., Al-Osta, M. (2020). Effect of sugar dosage on setting time, microstructure and strength of Type I and Type V Portland cements. Case Studies in Construction Materials, 13: e00364. https://doi.org/10.1016/j.cscm.2020.e00364
[6] Záleská, M., Pavlíková, M., Pavlík, Z., Jankovský, O., Pokorný, J., Tydlitát, V., Svora, P., Černý, R. (2018). Physical and chemical characterization of technogenic pozzolans for the application in blended cements. Construction and Building Materials, 160: 106-116. https://doi.org/10.1016/j.conbuildmat.2017.11.021
[7] Hossain, M.M., Karim, M.R., Hasan, M., Hossain, M.K., Zain, M.F.M. (2016). Durability of mortar and concrete made up of pozzolans as a partial replacement of cement: A review. Construction and Building Materials, 116: 128-140. https://doi.org/10.1016/j.conbuildmat.2016.04.147
[8] Sharbaf, M., Najimi, M., Ghafoori, N. (2022). A comparative study of natural pozzolan and fly ash: Investigation on abrasion resistance and transport properties of self-consolidating concrete. Construction and Building Materials, 346: 128330. https://doi.org/10.1016/j.conbuildmat.2022.128330
[9] Baueregger, S., Perello, M., Plank, J. (2015). Influence of carboxylated styrene-butadiene latex copolymer on Portland cement hydration. Cement and Concrete Composites, 63: 42-50. https://doi.org/10.1016/j.cemconcomp.2015.06.004
[10] Hale, W.M., Freyne, S.F., Bush Jr, T.D., Russell, B.W. (2008). Properties of concrete mixtures containing slag cement and fly ash for use in transportation structures. Construction and Building Materials, 22(9): 1990-2000. https://doi.org/10.1016/j.conbuildmat.2007.07.004
[11] Poornamazian, A., Izadinia, M. (2024). A comprehensive investigation of performance characteristics, mechanical properties and durability parameters of self-compacting concrete containing iron slag as coarse aggregate. Periodica Polytechnica Civil Engineering, 68(2): 498-510. https://doi.org/10.3311/PPci.22846
[12] Dhir, R.K., Byars, E.A. (1993). PFA concrete: Permeation properties of cover to steel reinforcement. Cement and Concrete Research, 23(3): 554-566. https://doi.org/10.1016/0008-8846(93)90005-T
[13] Ahmad, S., Al-Amoudi, O.S.B., Khan, S.M., Maslehuddin, M. (2022). Effect of silica fume inclusion on the strength, shrinkage and durability characteristics of natural pozzolan-based cement concrete. Case Studies in Construction Materials, 17: e01255. https://doi.org/10.1016/j.cscm.2022.e01255
[14] Samimi, K., Zareechian, M. (2022). Chemical resistance of synthesized graphene-modified cement paste containing natural pozzolans to acid attack. Journal of Building Engineering, 60: 105174. https://doi.org/10.1016/j.jobe.2022.105174
[15] Mohammed, S., Safiullah, O. (2018). Optimization of the SO3 content of an Algerian Portland cement: Study on the effect of various amounts of gypsum on cement properties. Construction and Building Materials, 164: 362-370. https://doi.org/10.1016/j.conbuildmat.2017.12.218
[16] Al-Dulaimi, M.A.M., Seyedi, M. (2023). Numerical analysis of geogrids and recycled concrete aggregate for stabilizing road embankments. Annales de Chimie-Science Des Materiaux, 47(4): 219-223. https://doi.org/10.18280/acsm.470404
[17] Aqel, M., Panesar, D.K. (2016). Hydration kinetics and compressive strength of steam-cured cement pastes and mortars containing limestone filler. Construction and Building Materials, 113: 359-368. https://doi.org/10.1016/j.conbuildmat.2016.03.031
[18] Abbou, S.B., Aalil, I., Cherkaoui, K. (2024). The impact of brick powder specific surface area on cement replacement in Mortar Mixes: A sustainable and cost-effective solution for the construction industry. Periodica Polytechnica Civil Engineering, 68(1): 141-154. https://doi.org/10.3311/PPci.22643
[19] Elakneswaran, Y., Owaki, E., Miyahara, S., Ogino, M., Maruya, T., Nawa, T. (2016). Hydration study of slag-blended cement based on thermodynamic considerations. Construction and Building Materials, 124: 615-625. https://doi.org/10.1016/j.conbuildmat.2016.07.138
[20] Austin, J.B. (1939). Kinetics of the decomposition of austenite at constant temperature. Transactions of the American Institute of Mining and Metallurgical Engineers, 135: 396-415. https://ci.nii.ac.jp/naid/10007761998.
[21] Erdoğan, S.T., Koçak, T.Ç. (2017). Influence of slag fineness on the strength and heat evolution of multiple-clinker blended cements. Construction and Building Materials, 155: 800-810. https://doi.org/10.1016/j.conbuildmat.2017.08.120
[22] Knop, Y., Peled, A., Cohen, R. (2014). Influences of limestone particle size distributions and contents on blended cement properties. Construction and Building Materials, 71: 26-34. https://doi.org/10.1016/j.conbuildmat.2014.08.004
[23] Liu, Z., El-Tawil, S., Hansen, W., Wang, F. (2018). Effect of slag cement on the properties of ultra-high performance concrete. Construction and Building Materials, 190: 830-837. https://doi.org/10.1016/j.conbuildmat.2018.09.173
[24] Zine EL abidine, B., Salah, B., Noureddine, B., Ralida, Z.F., Djamel, T. (2019). Effect of coal additives on the physical and chemical properties of the Portland cement. International Journal of Coal Preparation and Utilization, 39(2): 55-64. https://doi.org/10.1080/19392699.2018.1518902
[25] Bentaieb, N., Benarima, Z.E.A., Belaadi, S. (2020). Calorimetric and thermal analysis studies on the influence of coal on cement paste hydration. Iranian Journal of Chemistry and Chemical Engineering, 39(6): 237-244. https://doi.org/10.30492/ijcce.2019.36706
[26] Bentaieb, N., Lachemet, A., Zirour, R., Belaadi, S., Frances, C. (2011). Thermal analysis of composite cements. Chemical Engineering Transactions, 24: 685-690. https://doi.org/10.3303/CET1124115
[27] Lila, K., Belaadi, S., Solimando, R., Zirour, F.R. (2020). Valorisation of organic waste: Use of olive kernels and pomace for cement manufacture. Journal of Cleaner Production, 277: 123703. https://doi.org/10.1016/j.jclepro.2020.123703
[28] Touil, D., Belaadi, S., Frances, C. (2006). Energy efficiency of cement finish grinding in a dry batch ball mill. Cement and Concrete Research, 36(3): 416-421. https://doi.org/10.1016/j.cemconres.2005.12.005

[29] Gupta, S., Mohapatra, B.N., Bansal, M. (2022). Development of Portland limestone cement (PLC) in India using different composition of cement and marginal grade limestone: A sustainable approach. Journal of the Indian Chemical Society, 99(11): 100724. https://doi.org/10.1016/j.jics.2022.100724

[30] Turanli, L., Uzal, B., Bektas, F. (2005). Effect of large amounts of natural pozzolan addition on properties of blended cements. Cement and Concrete Research, 35(6): 1106-1111. https://doi.org/10.1016/j.cemconres.2004.07.022

[31] Hamdi, O.M., Ahmed-Chaouch, A., Saïdani, M., Alioui, H. (2023). Use of the Algerian natural pozzolan for the production of a geopolymer as a complete cement replacement. Construction and Building Materials, 400(7): 132723. https://doi.org/10.1016/j.conbuildmat.2023.132723

[32] Briki, Y., Zajac, M., Haha, M.B., Scrivener, K. (2021). Impact of limestone fineness on cement hydration at early age. Cement and Concrete Research, 147(6): 106515. https://doi.org/10.1016/j.cemconres.2021.106515

[33] Boubekeur, T., Boulekbache, B., Aoudjane, K., Ezziane, K., Kadri, E.H. (2019). Prediction of the durability performance of ternary cement containing limestone powder and ground granulated blast furnace slag. Construction and Building Materials, 209: 215-221. https://doi.org/10.1016/j.conbuildmat.2019.03.120

[34] Elkhadiri, I., Puertas, F. (2008). The effect of curing temperature on sulphate-resistant cement hydration and strength. Construction and Building Materials, 22(7): 1331-1341. https://doi.org/10.1016/j.conbuildmat.2007.04.014

[35] Diab, A.M., Abd Elmoaty, M., Aly, A.A. (2016). Long term study of mechanical properties, durability and environmental impact of limestone cement concrete. Alexandria Engineering Journal, 55(2): 1465-1482. https://doi.org/10.1016/j.aej.2016.01.031

[36] Panghal, H., Kumar, A. (2024). Sustainable concrete: Exploring fresh, mechanical, durability, and microstructural properties with recycled fine aggregates. Periodica Polytechnica Civil Engineering, 68(2): 543-558. https://doi.org/10.3311/PPci.22711

[37] Chen, T.T., Wang, C.C., Hsiung, B.B., Wang, H.Y. (2017). Seven-day test result assessment of the developed strength in composite cement mortar with slag. Construction and Building Materials, 152: 587-597. https://doi.org/10.1016/j.conbuildmat.2017.07.001

[38] Dai, S., Zhu, H., Zhang, D., Liu, Z., Cheng, S., Zhao, J. (2022). Insights to compressive strength, impermeability and microstructure of micro-expansion steel slag cement under constraint conditions. Construction and Building Materials, 326: 126540. https://doi.org/10.1016/j.conbuildmat.2022.126540

[39] Ghrici, M., Kenai, S., Said-Mansour, M. (2007). Mechanical properties and durability of mortar and concrete containing natural pozzolana and limestone blended cements. Cement and Concrete Composites, 29(7): 542-549. https://doi.org/10.1016/j.cemconcomp.2007.04.009

[40] Lollini, F., Redaelli, E., Bertolini, L. (2014). Effects of portland cement replacement with limestone on the properties of hardened concrete. Cement and Concrete Composites, 46: 32-40. https://doi.org/10.1016/j.cemconcomp.2013.10.016

[41] Boughamsa, O., Abdelouahed, A., Hebhoub, H., Kherraf, L., Boukhatem, G. (2023). Optimizing sand concrete properties through partial substitution of natural sand with cement kiln dust. Annales de Chimie Science des Matériaux, 47(4): 259-264. https://doi.org/10.18280/acsm.470408

[42] Königsberger, M., Carette, J. (2020). Validated hydration model for slag-blended cement based on calorimetry measurements. Cement and Concrete Research, 128: 105950. https://doi.org/10.1016/j.cemconres.2019.105950

[43] Wang, Y., Shui, Z., Wang, L., Gao, X., Huang, Y., Song, Q., Liu, K. (2020). Alumina-rich pozzolan modification on Portland-limestone cement concrete: Hydration kinetics, formation of hydrates and long-term performance evolution. Construction and Building Materials, 258: 119712. https://doi.org/10.1016/j.conbuildmat.2020.119712

[44] Celik, K., Hay, R., Hargis, C.W., Moon, J. (2019). Effect of volcanic ash pozzolan or limestone replacement on hydration of Portland cement. Construction and Building Materials, 197: 803-812. https://doi.org/10.1016/j.conbuildmat.2018.11.193

[45] Ulusu, H., Aruntaş, H.Y., Gültekin, A.B., Dayı, M., Çavuş, M., Kaplan, G. (2023). Mechanical, durability and microstructural characteristics of Portland pozzolan cement (PPC) produced with high volume pumice: Green, cleaner and sustainable cement development. Construction and Building Materials, 378: 131070. https://doi.org/10.1016/j.conbuildmat.2023.131070

[46] de Siqueira, A.A., Cordeiro, G.C. (2022). Properties of binary and ternary mixes of cement, sugarcane bagasse ash and limestone. Construction and Building Materials, 317: 126150. https://doi.org/10.1016/j.conbuildmat.2021.126150

[47] Scherer, G.W., Zhang, J., Thomas, J.J. (2012). Nucleation and growth models for hydration of cement. Cement and Concrete Research, 42(7): 982-993. https://doi.org/10.1016/j.cemconres.2012.03.019

[48] Zemri, C., Bouiadjra, M.B. (2023). Thermal impact on the physical and transfer properties of slag cement and Portland cement concretes. Annales de Chimie Science des Matériaux, 47(6): 371-381. https://doi.org/10.18280/acsm.470603

[49] Wang, X.Y. (2018). Analysis of hydration and strength optimization of cement-fly ash-limestone ternary blended concrete. Construction and Building Materials, 166: 130-140. https://doi.org/10.1016/j.conbuildmat.2018.01.058

[50] Medjigbodo, G., Rozière, E., Charrier, K., Izoret, L., Loukili, A. (2018). Hydration, shrinkage, and durability of ternary binders containing Portland cement, limestone filler and metakaolin. Construction and Building Materials, 183: 114-126. https://doi.org/10.1016/j.conbuildmat.2018.06.138

[51] Hallet, V., Pedersen, M.T., Lothenbach, B., Winnefeld, F., De Belie, N., Pontikes, Y. (2022). Hydration of blended cement with high volume iron-rich slag from non-ferrous metallurgy. Cement and Concrete Research, 151: 106624. https://doi.org/10.1016/j.cemconres.2021.106624

[52] D'aloia, L., Chanvillard, G. (2002). Determining the “apparent” activation energy of concrete: Ea-numerical

simulations of the heat of hydration of cement. Cement and Concrete Research, 32(8): 1277-1289. https://doi.org/10.1016/S0008-8846(02)00791-3
[53] Snellings, R., Machner, A., Bolte, G., Kamyab, H., Durdzinski, P., Teck, P., Zajac, M., Muller, A., de Weerdt, K., Haha, M.B. (2022). Hydration kinetics of ternary slag-limestone cements: Impact of water to binder ratio and curing temperature. Cement and Concrete Research, 151: 106647. https://doi.org/10.1016/j.cemconres.2021.106647